Electronic Supplementary Information

Reactivity of the Bifunctional Ambiphilic Molecule 8-(dimesitylboryl)quinoline : Hydrolysis and Coordination to Cu^{I}, Ag^{I} and Pd^{II}

*Jung-Ho Son, Michael A. Pudenz, James D. Hoefelmeyer**

Department of Chemistry, The University of South Dakota, 414 E. Clark St., Vermillion, SD 57069

* Author contact: jhoefelm@usd.edu

Synthesis of 8-iodoquinoline.

Modifications from the references were made for better yield.[1] 8-aminoquinoline (10 g, 0.069 mol, Aldrich), water (30 ml), ice (60 g) and concentrated HCl (30 ml) was stirred in 600ml beaker and cooled in an ice bath, which formed red solution. An ice-cooled $NaNO_2$ (5.18 g, 0.075 mol, Fischer) solution in water (30 ml) was added to the 8-aminoquinoline solution portionwise with stirring. The addition was stopped at the point when tiny bubbles formed at the surface of the solution. After stirring 10 min in an ice bath, KI (12.45 g, 0.075 mol, Aldrich) dissolved in water (25 ml) was added to the reaction mixture portionwise. Large bubbles formed during the addition. The solution turned to dark brown and stirred overnight. The solution was briefly heated up for 10 min with a watch glass on top of the beaker. After cooling, the mixture was neutralized by NaOH, until the solution turned to basic. During NaOH addition, light brown oil formed at the bottom of the beaker. The solution was stood still until the oil settled down. The supernatant was removed, and remaining oil was purified by vacuum distillation, which gave 14.8g (84 %) of 8-iodoquinoline as a yellow-orange oil.

1 (a) Lucas, H. J., Kennedy, E. R., *Org. Synth. Coll. Vol. II*, 1943, 351. (b) Son, J. -H., Hoefelmeyer, J. D., *Acta Cryst.* 2008, **E64**, o2076. (c) Son, J. -H., Hoefelmeyer, J. D., *Acta Cryst.* 2008, **E64**, o2077.

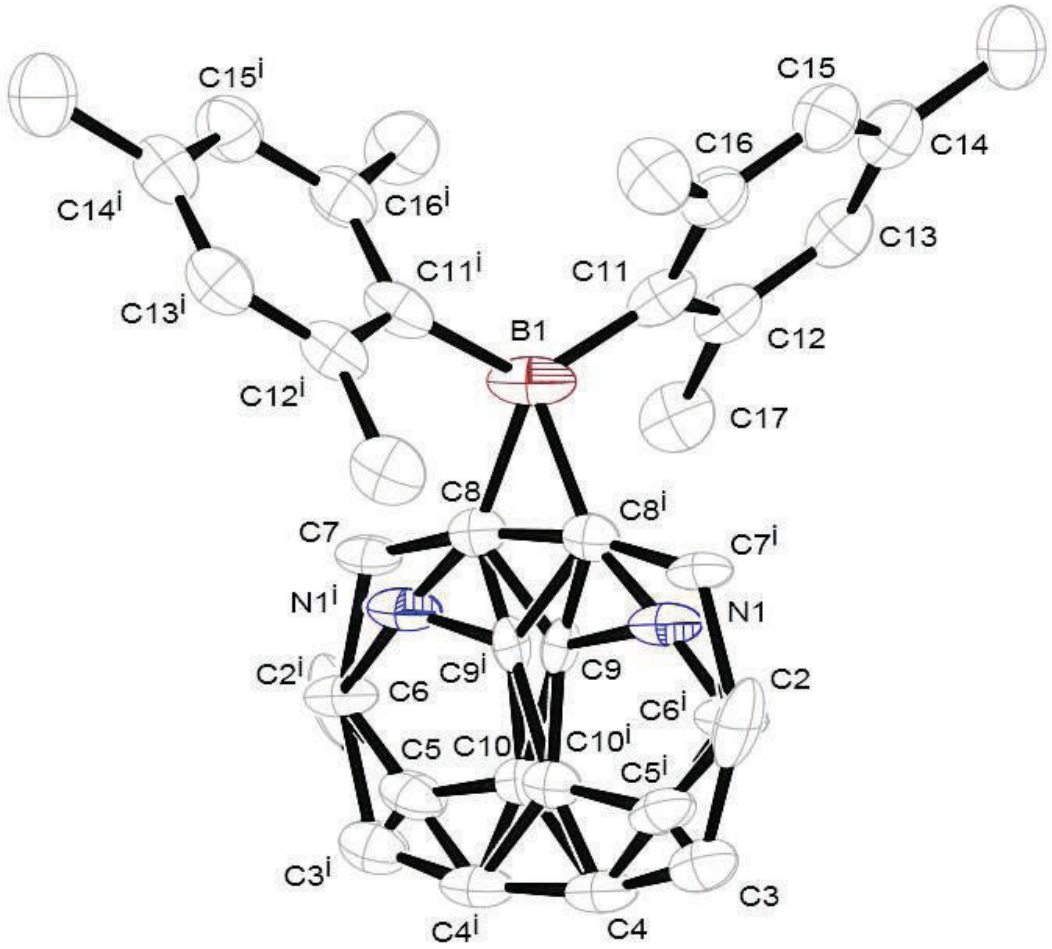

Fig. S1 Stucture of **1a** in the crystal. Selected bond lengths (Å) and angles (deg): C(8)-B(1) = 1.653(7), C(11)-B(1) = 1.564(4), C(9)-C(8)-B(1) = 115.2(4), C(7)-C(8)-B(1) = 125.8(5), $C(11)^{i}$-B(1)-C(8) = 103.5(2), C(11)-B(1)-C(8) = 131.6(3), $C(11)^{i}$-B(1)-C(11) = 121.3(4). i = -x,y,-z+3/2

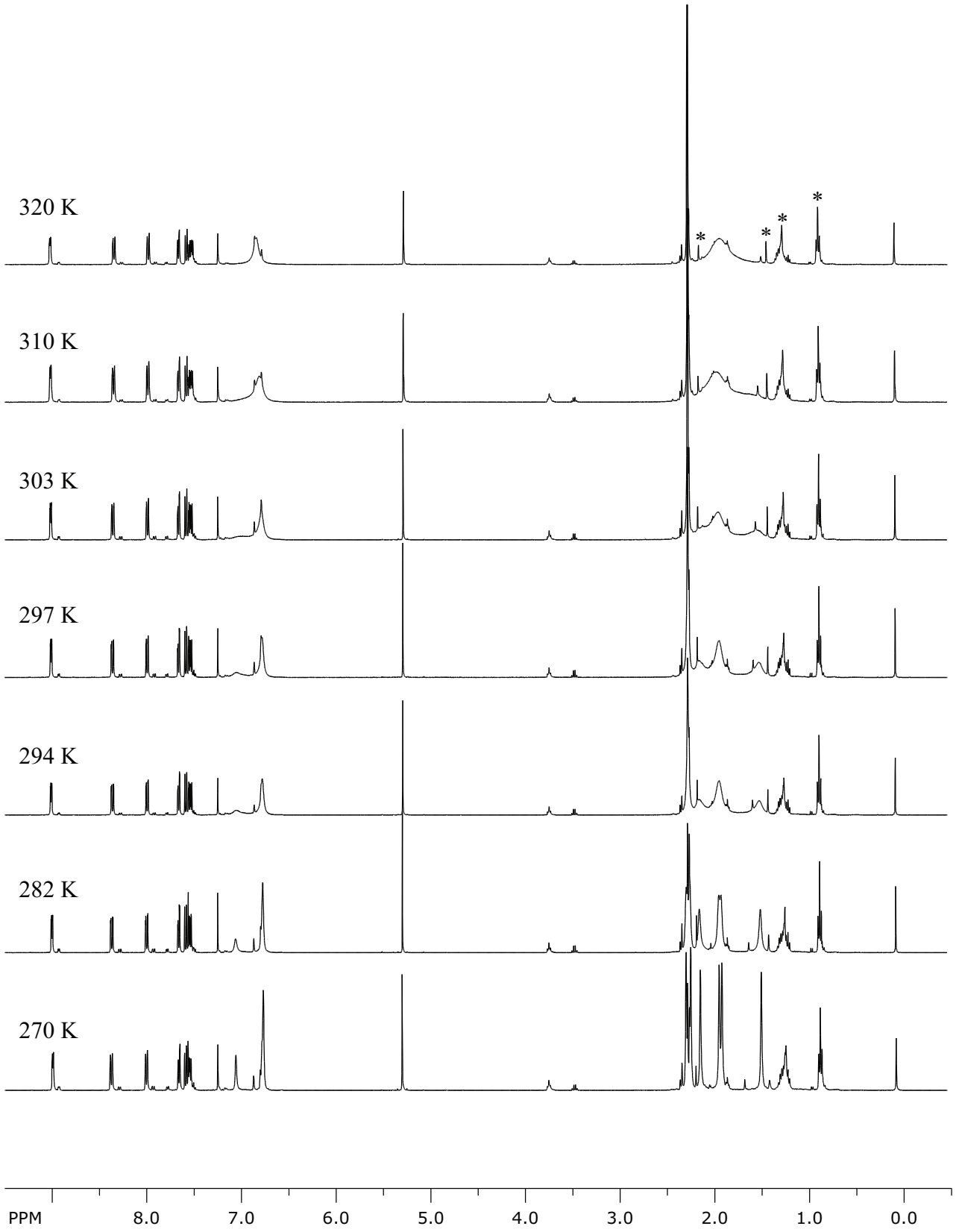

Fig. S2 VT ^{1}H NMR data of **5** (impurities are marked with *).

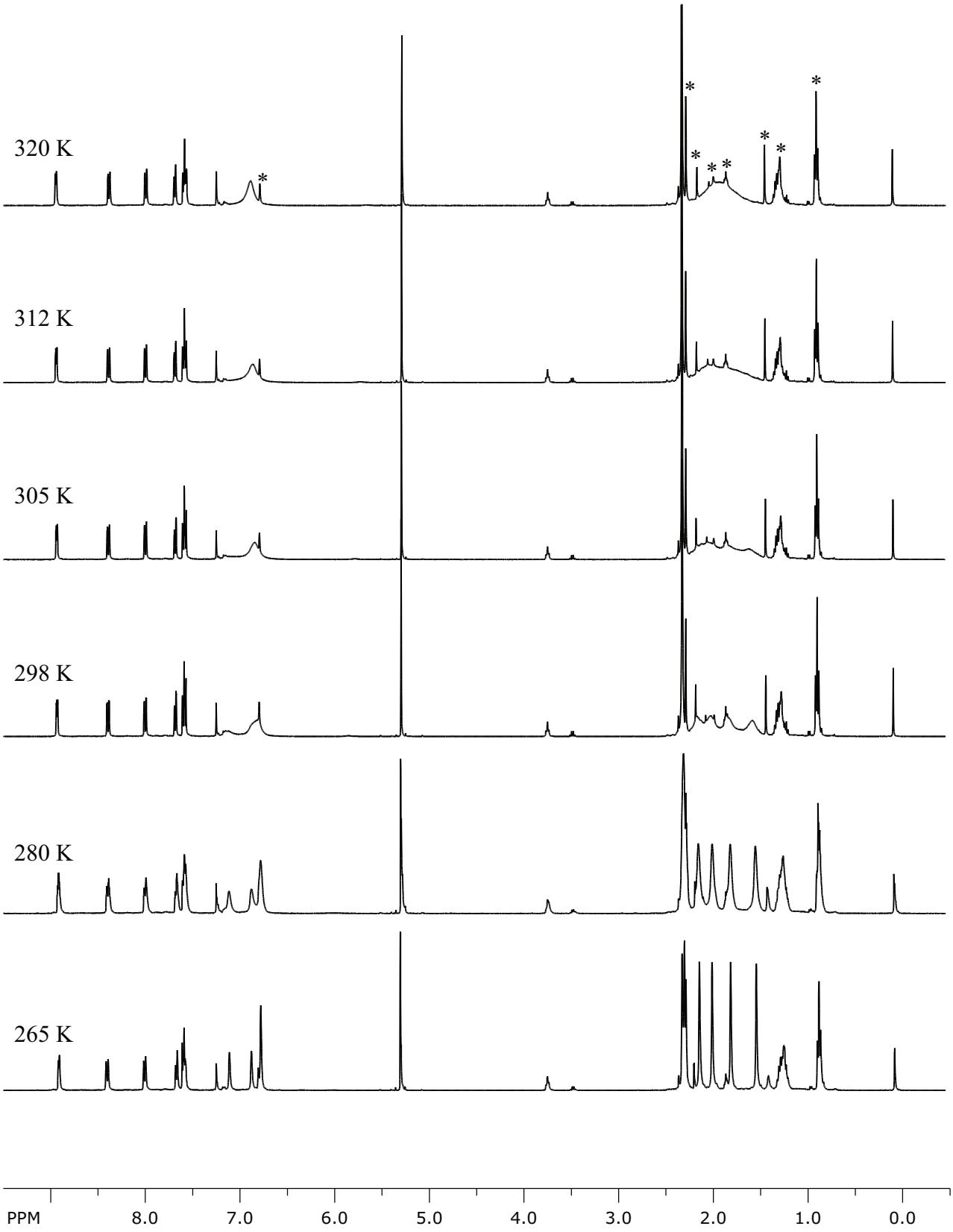

Fig. S3 VT ^{1}H NMR data of **6** (impurities are marked with *).

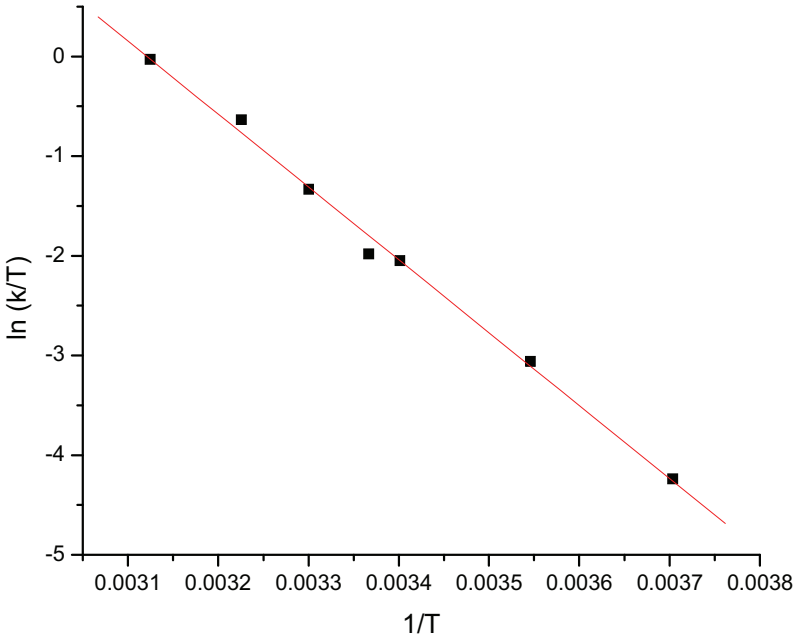

Fig. S4 Eyring plot of the exchange rate of *o*-CH_3(Mes) peaks by line shape analysis of the VT ^{1}H NMR data of **5**.

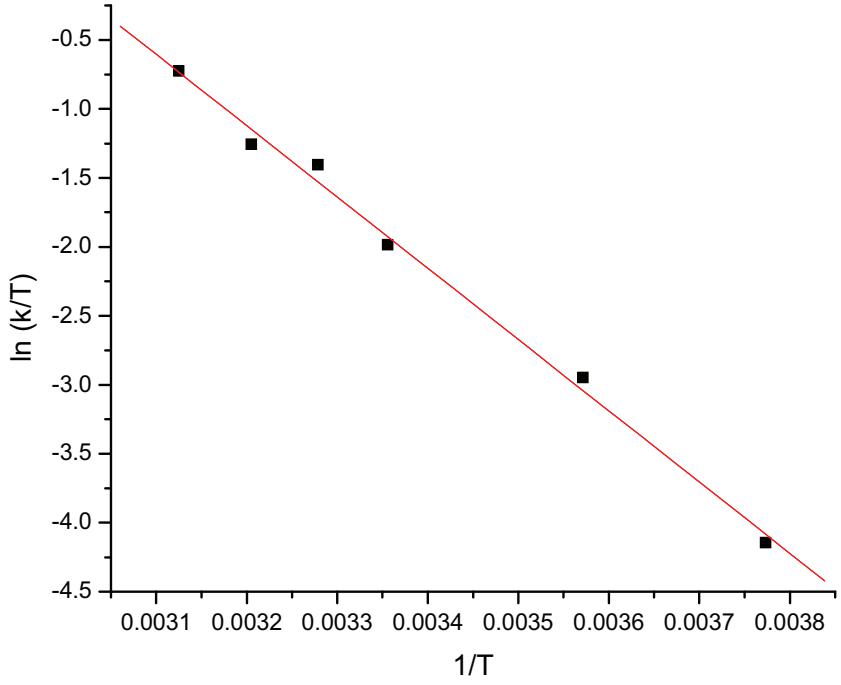

Fig. S5 Eyring plot of the exchange rate of *o*-CH_3Mes) peaks by line shape analysis of the VT ^{1}H NMR data of **6**.

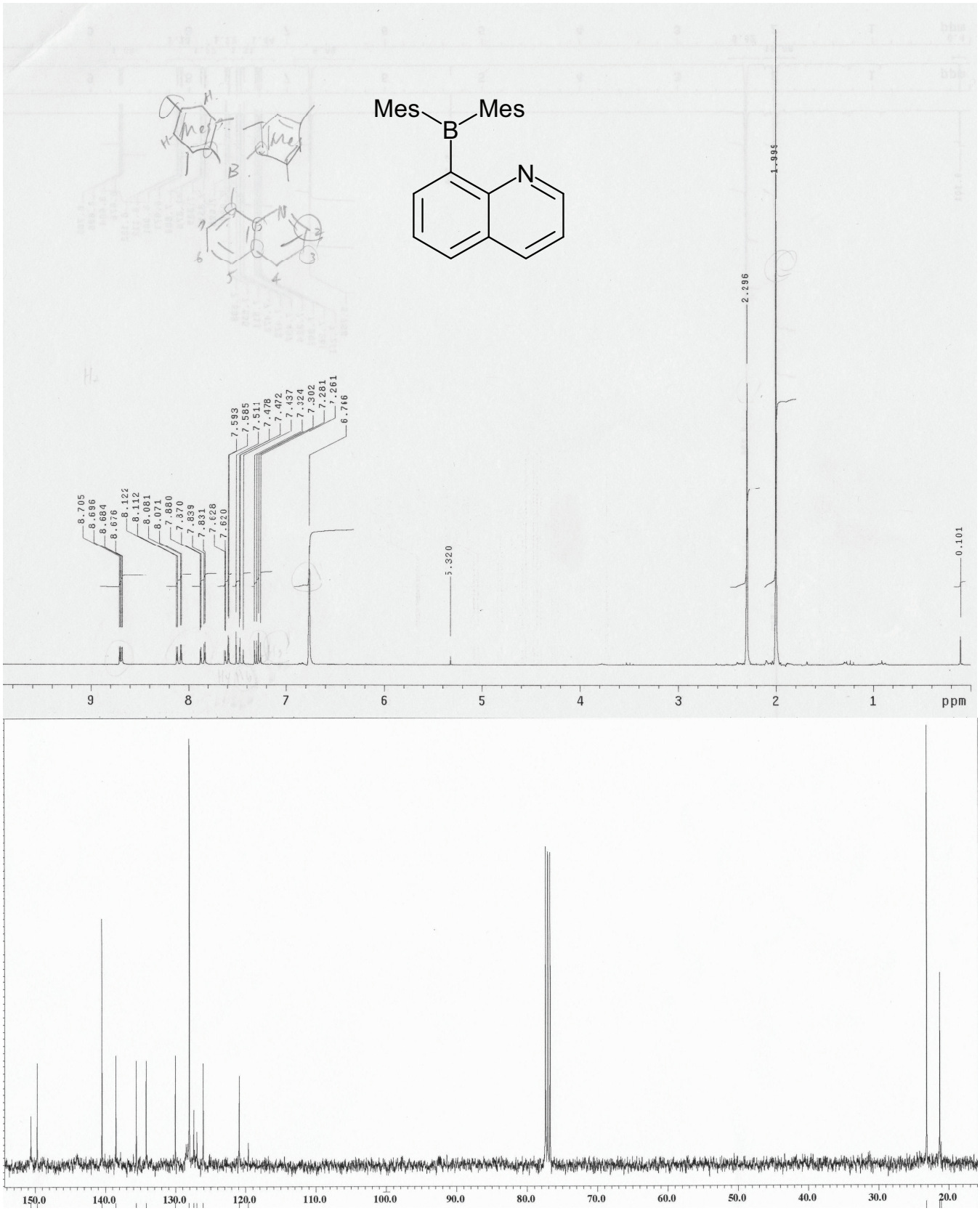

Fig. S6 ^{1}H (upper, 200 MHz) and ^{13}C (lower, 100 MHz) NMR spectra of **1** in $CDCl_3$.

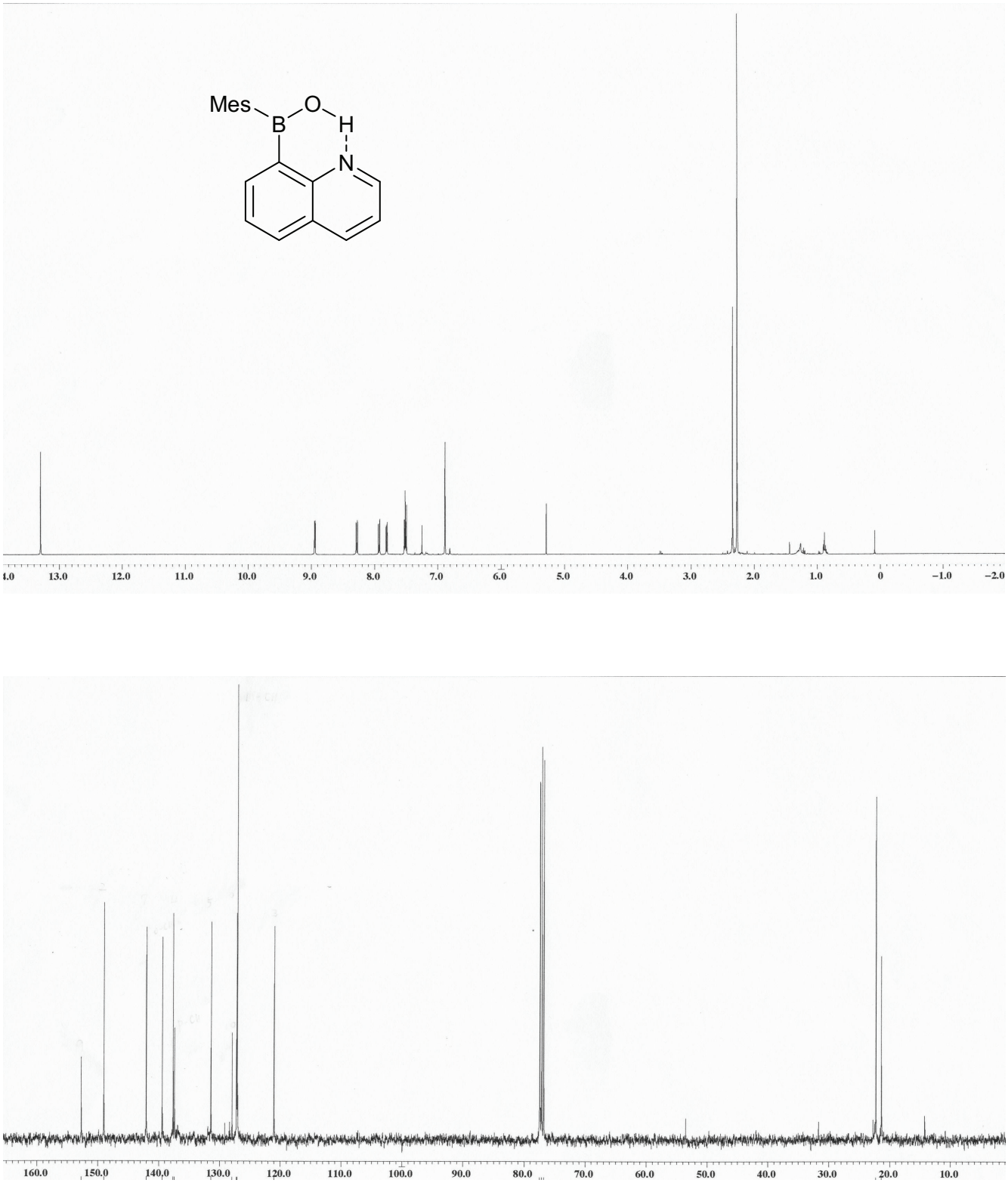

Fig. S7 ^{1}H (upper, 400 MHz) and ^{13}C (lower, 100 MHz) NMR spectra of **2** in $CDCl_3$.

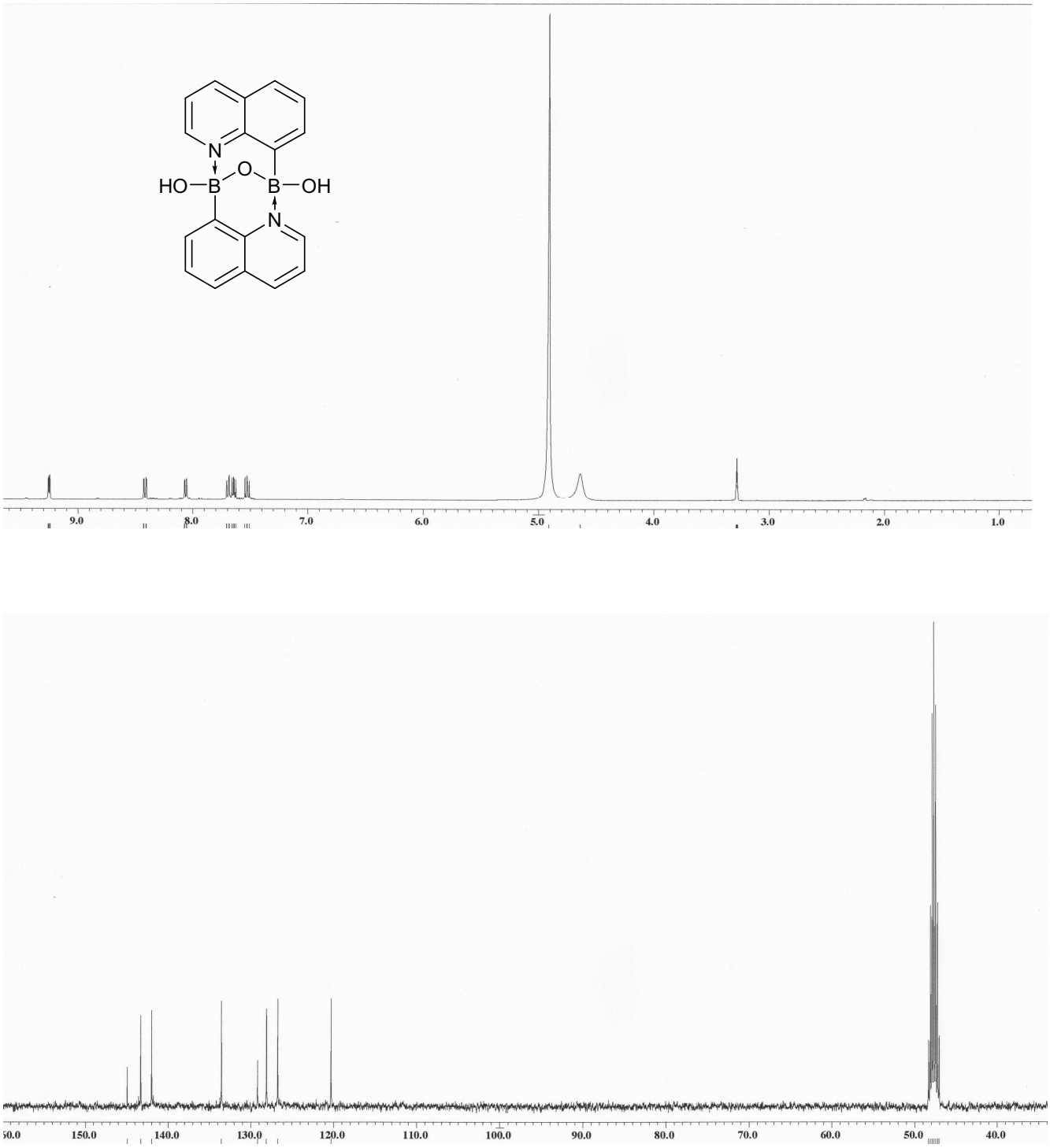

Fig. S8 ^{1}H (upper, 400 MHz) and ^{13}C (lower, 100 MHz) NMR spectra of **3** in CD_3OD.

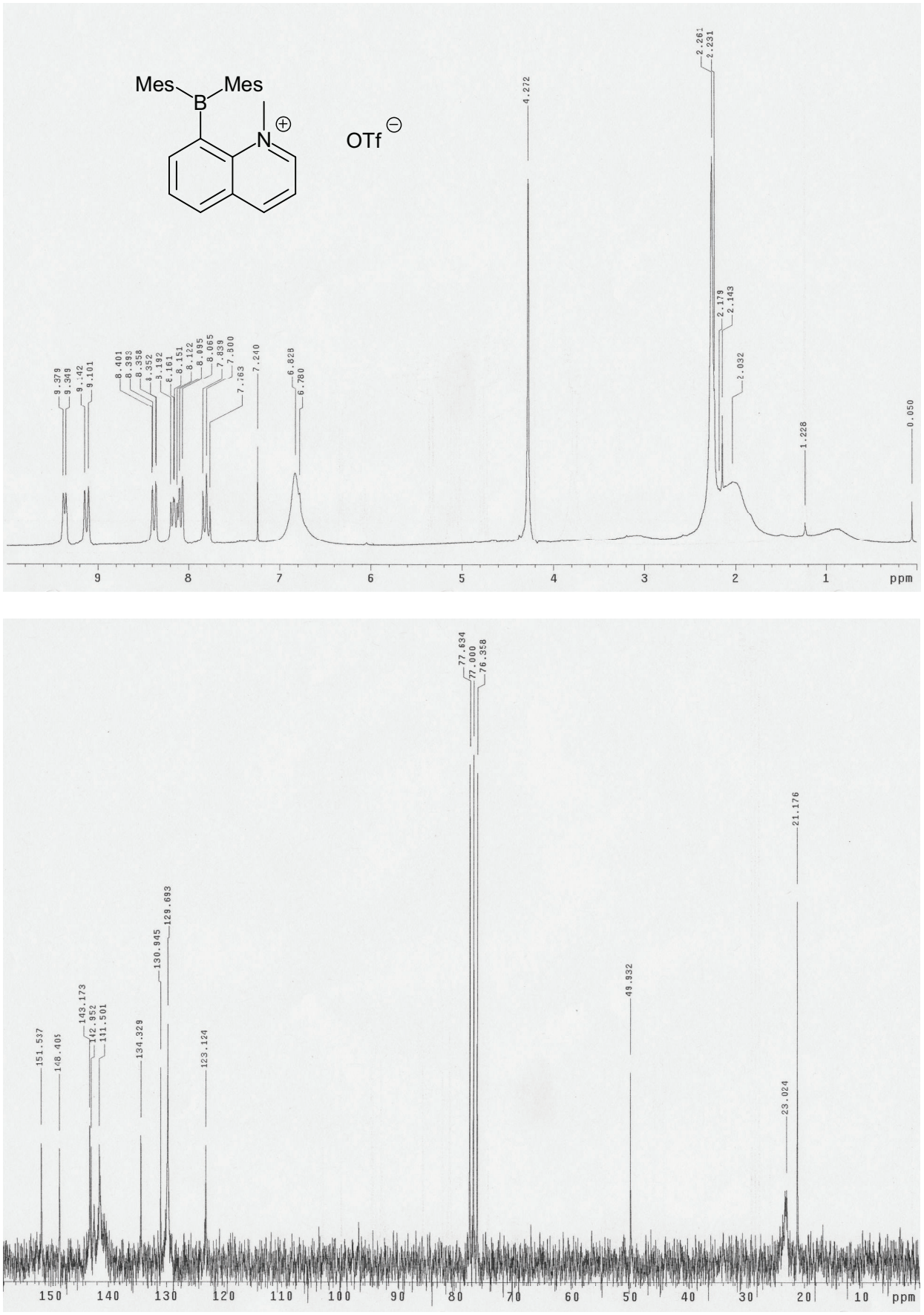

Fig. S9 ^{1}H (upper, 200 MHz) and ^{13}C (lower, 50 MHz) NMR spectra of **4** in $CDCl_3$.

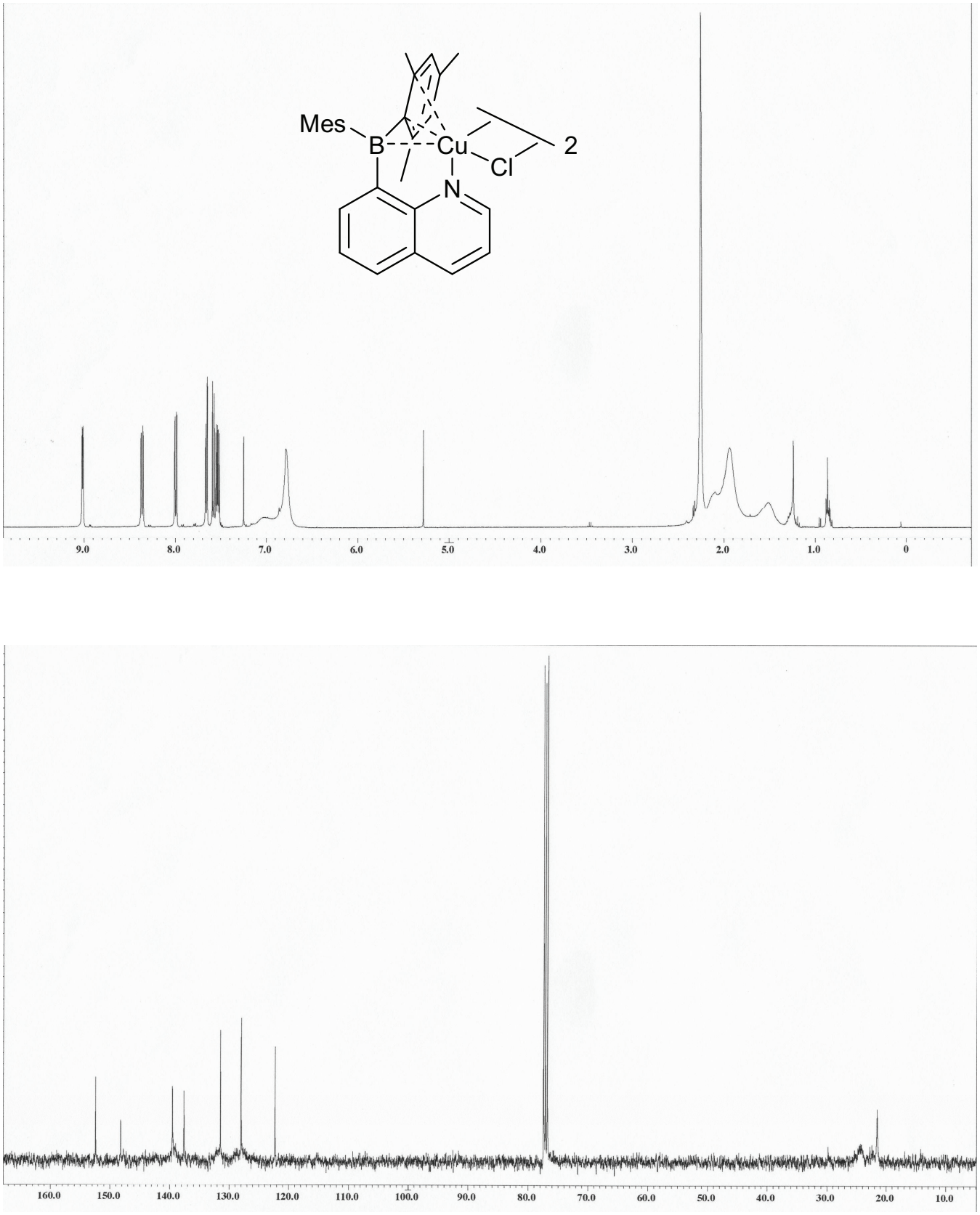

Fig. S10 ^{1}H (upper, 400 MHz) and ^{13}C (lower, 100 MHz) NMR spectra of **5** in $CDCl_3$.

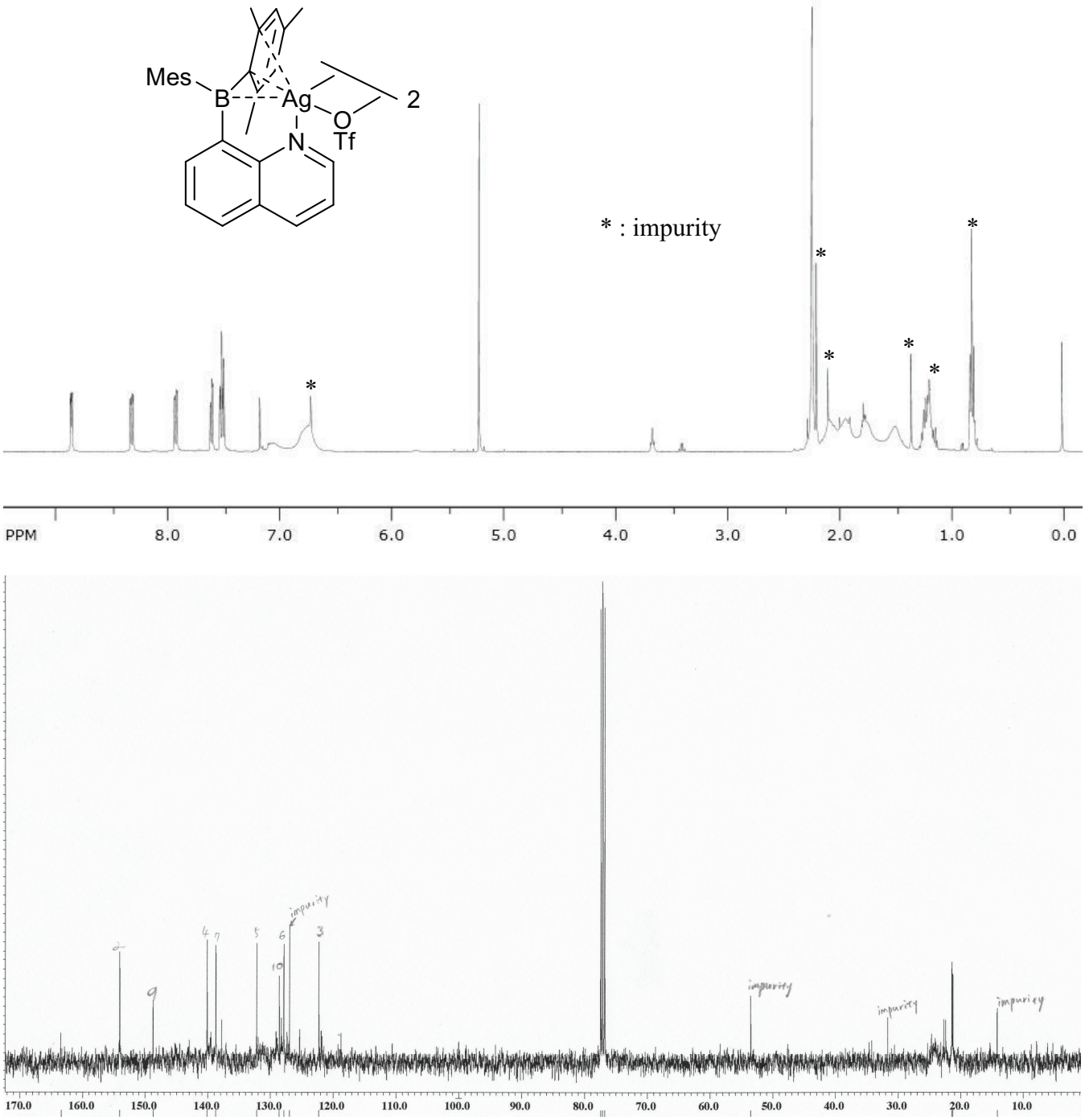

Fig. S11 ^{1}H (upper, 400 MHz) and ^{13}C (lower, 100 MHz) NMR spectra of **6** in $CDCl_3$.

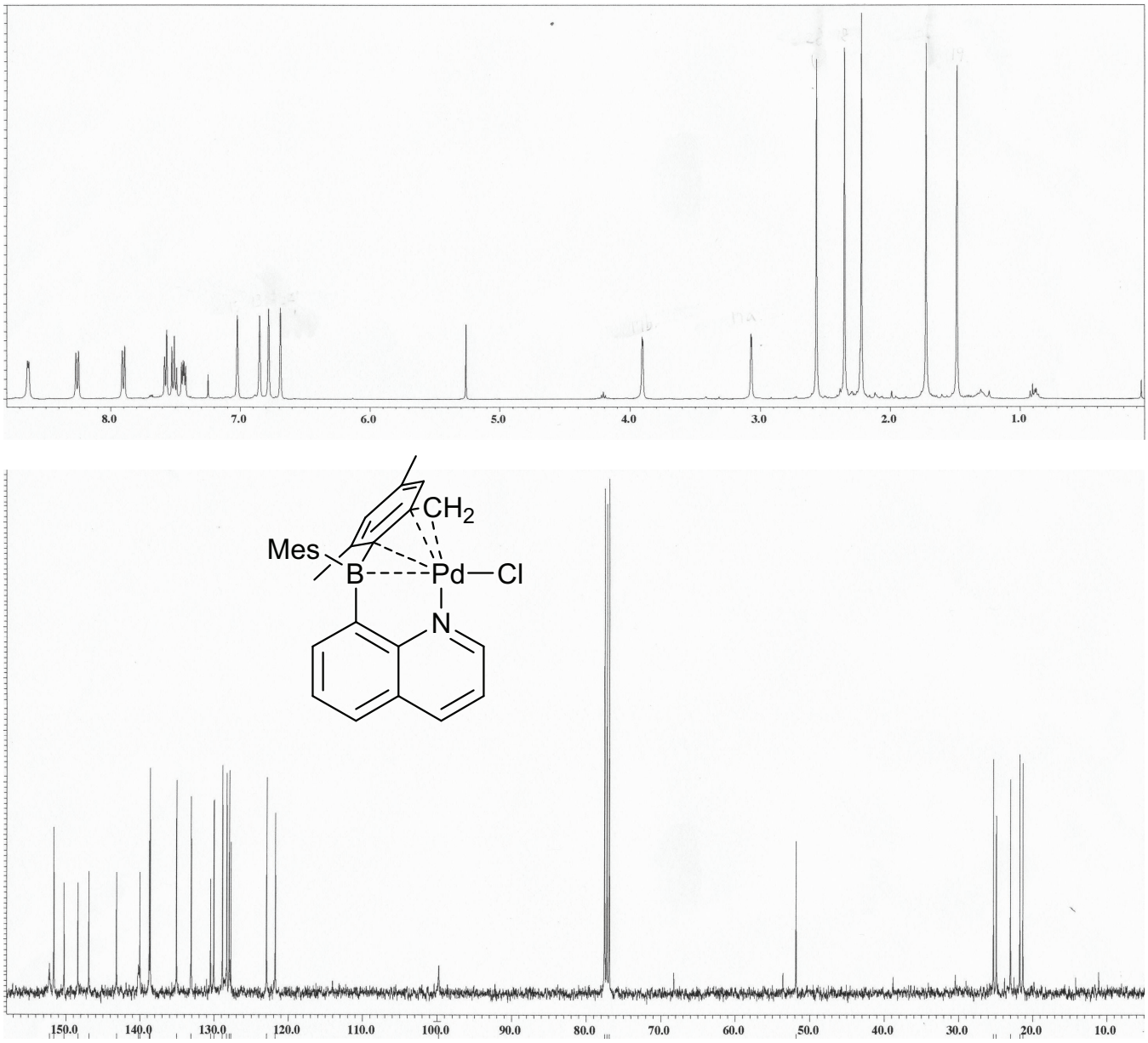

Fig. S12 ^{1}H (upper, 400 MHz) and ^{13}C (lower, 100 MHz) NMR spectra of **7** in $CDCl_3$.